CHARTER IV

RESULTS

1. Sequence analysis in the *BTK* gene

1.1 Sequence analysis in the *Bruton's tyrosine kinase* cDNA

Sequence analysis of the *BTK* cDNA from the six unrelated patients with XLA identified five disease-causing mutations. There are five different sequence variants including three novel ones.

Patient 1: A boy presenting with XLA was found to have a novel frameshift mutation caused by a deletion of a thymine at nucleotide position 400 (c.400delT) (Fig. 14). This alteration is expected to result in changing the tyrosine to threonine at position 134, subsequent changes of 63 amino acids and truncation at amino acid 198 (Y134TfsX198).

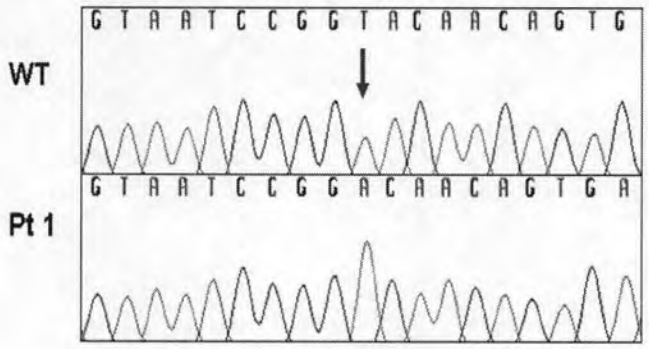

Figure 13: Direct sequencing of the *BTK* gene reveals that the patient is hemizygous for the c. 400delT (Y134TfsX198) mutation.

Patient 2: A boy presenting with XLA was found to have a frameshift mutation caused by a deletion of a guanine at nucleotide position 655 (c.655delG) (Fig. 15). This alteration is expected to result in changing the valine to leucine at position 219, subsequent changes of 8 amino acids and truncation at amino acid 228 (V219LfsX228).

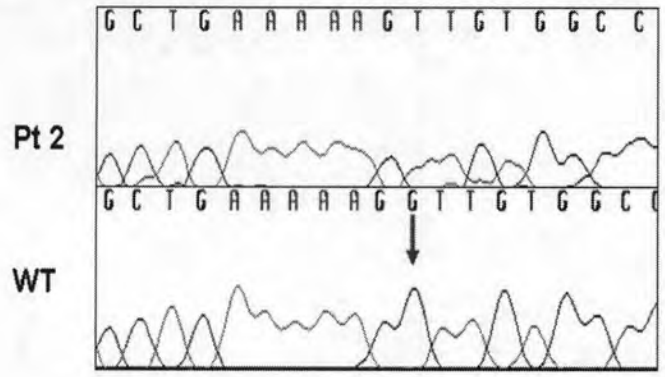

Figure 14: Direct sequencing of the *BTK* gene reveals that the patient is hemizygous for the c. c.655delG (V219LfsX228) mutation. The mutation has been previously reported in a patient affected with this disease (*Keiko et al.*, Blood 2000).

Patient 3: A boy presenting with XLA was found to have a novel missense mutation. He was hemizygous for a T to A mutation at nucleotide position 1415 (c.1415T>A) (Fig. 16). The mutation is expected to result in an isoleucine to asparagine substitution at codon 472 (p.I472N).

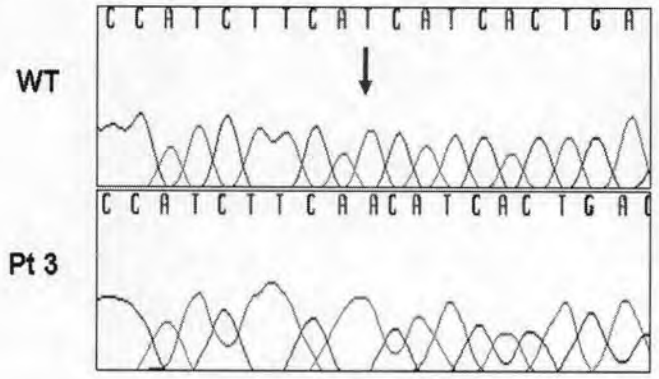

Figure 15: Direct sequencing of the *BTK* gene reveals that the patient is hemizygous for the c. c.1415T>A (p.I472N) mutation.

Patient 4: A boy was found to have a missense mutation. He was hemizygous for a G to A transition at nucleotide position 1922 (c.1922G>A) (Fig. 17). The mutation is expected to result in an arginine to histidine substitution at codon 641 (p.R641H).

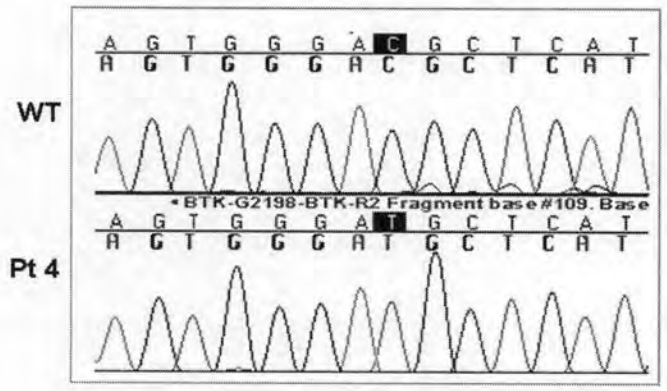

Figure 16: Direct sequencing of the *BTK* gene (using a reverse primer) reveals that the patient is hemizygous for the c.1922G>A (p.R641H) mutation. The mutation has been previously reported in a patient affected with this disease (*Jin et al.*, Hum Mol Genet 1995)

Patient 5: A boy presenting with XLA was found to have a novel splicing mutation resulting in an insertion of 106 base pairs into the mRNA transcript between exons 3 and 4 (Fig. 18).

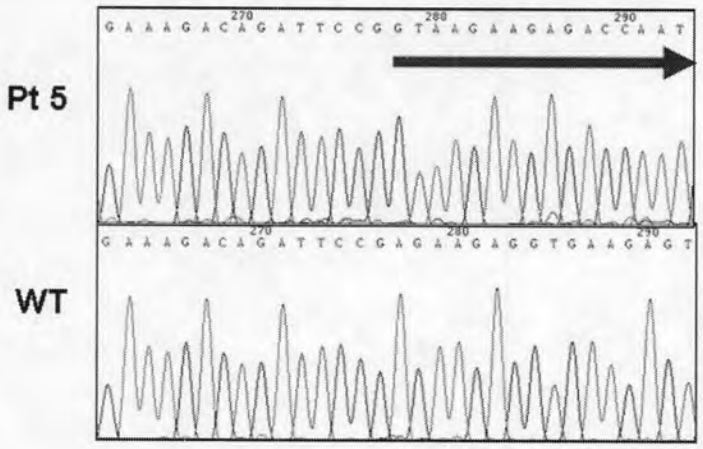

Figure 17: Direct sequencing of the *BTK* cDNA reveals that the patient is hemizygous for the 106 bp-insertion between exons 3 and 4.

1.2 Sequence analysis in the *Bruton's tyrosine kinase* genomic DNA

Patient 5: PCR-sequencing analysis of a part of intron 3 revealed that the patient was hemizygous for a c.240+109 C>A (IVS3+109 C>A) mutation (Fig. 19).

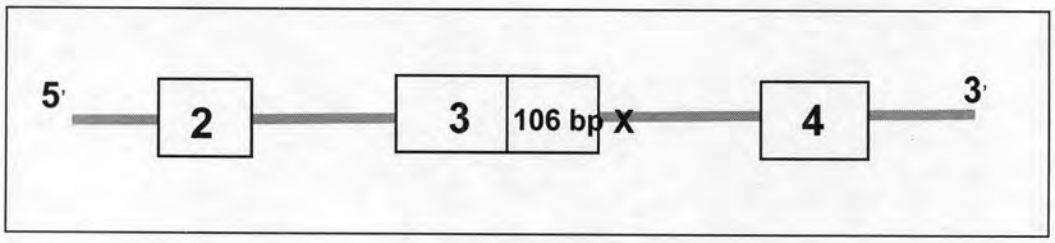

Figure 18: Schematic representation of the *BTK* coding region with the pseudoexon. Exons and pseudoexon are boxed. A splice site mutation at c.240+109 C>A was located at intron 3..

A summary of XLA patients with mutations in the *BTK* gene is shown in table 12.

Table 12: Conclusion of mutations identified in the *BTK* gene

Patient	Nucleotide change	Amino acid change	Exon/Intron/Domain
P 1	c.400delT	Y134TfsX198	Exon 3/ PH domain
P 2	c.655delG	V219LfsX228	Exon 6/ TH domain
P 3	c.1415T>A	I472N	Exon 14/ PH domain
P 4	c.1922G>A	R641H	Exon 18/ kinase domain
P 5	c.240+109 C>A	Insert pseudoexon	Intron 3/ PH domain
P 6	not found	-	-

2. AMOs administration in the patient's PBMCs

RT-PCR of the blood samples from the patient with a c.240+109 C>A mutation revealed a 274-bp product representing the aberrantly splicing. The correct spliced product contains 168 base pairs (Fig. 20).

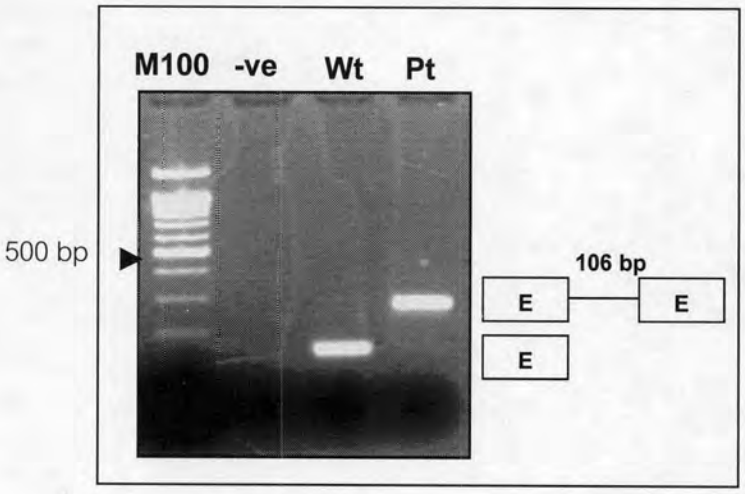

Figure 19: The results of the RT-PCR analysis using indicated primers (table 3) are shown along with a schematic representation of the transcripts obtained. M = 100-bp marker; –VE = negative control (no template), Wt = RNA sample from an unaffected control; Pt = the patient's untreated PBMCs. E = exon

2.1 AMOs optimization

The correctly-spliced *BTK* mRNA was restored in PBMC cultures using the target AMOs specifically designed to block aberrant splicing. The AMOs used were complementary to the splice site mutation of the intronic sequences (fig. 12), thereby blocking an access of the splicing machinery to the pre-mRNA.

The correctly spliced fragment was generated 24 h after administration of the AMOs together with the endo-porter carrier into the PBMC cultures. The products of aberrant splicing were still present. The correctly-spliced products persist after 72 h of AMOs administration. In untreated cell lines, practically no correctly spliced mRNA was detected, as shown by the lack of wide-type band.

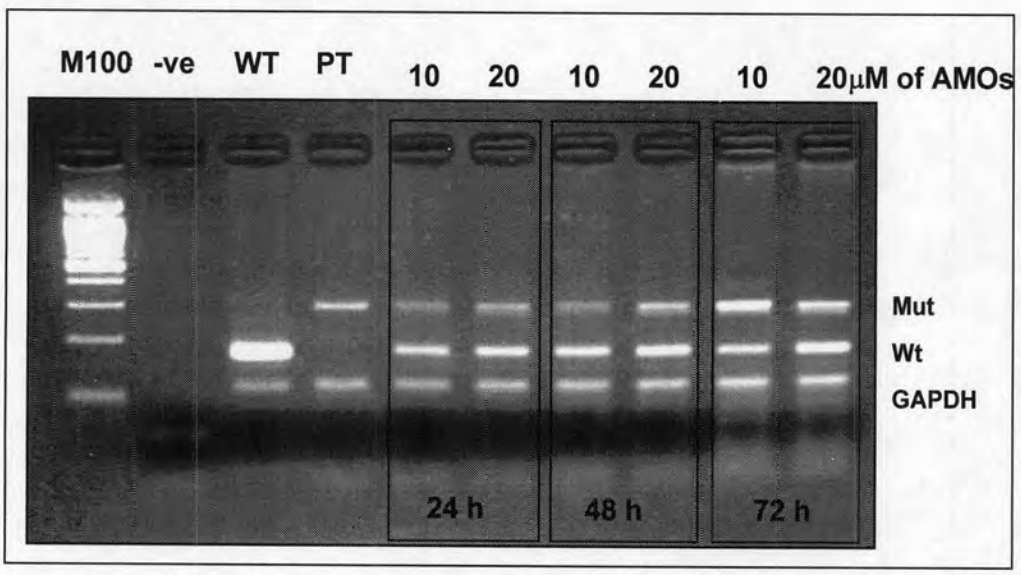

Figure 20: Correction of aberrant splicing of the *BTK* mRNA in PBMCs after AMOs administration. Cells were treated with two concentrations (10μM, 20μM) of the target AMOs. Total

RNA samples were collected at 24, 48 and 72 h after AMOs administration and analyzed by RT-PCR. –VE = negative control (no template), Wt = RNA sample from unaffected control, Pt = the patient's untreated PBMCs.

2.2 Variation of AMOs concentration

RT-PCR analysis of total RNA isolated 24 h after AMOs administration was performed in all tested samples. The levels of correctly spliced *BTK* mRNA were not much different in cells treated with 10 to 60 μM of AMOs. The aberrant RNA bands are also apparent.

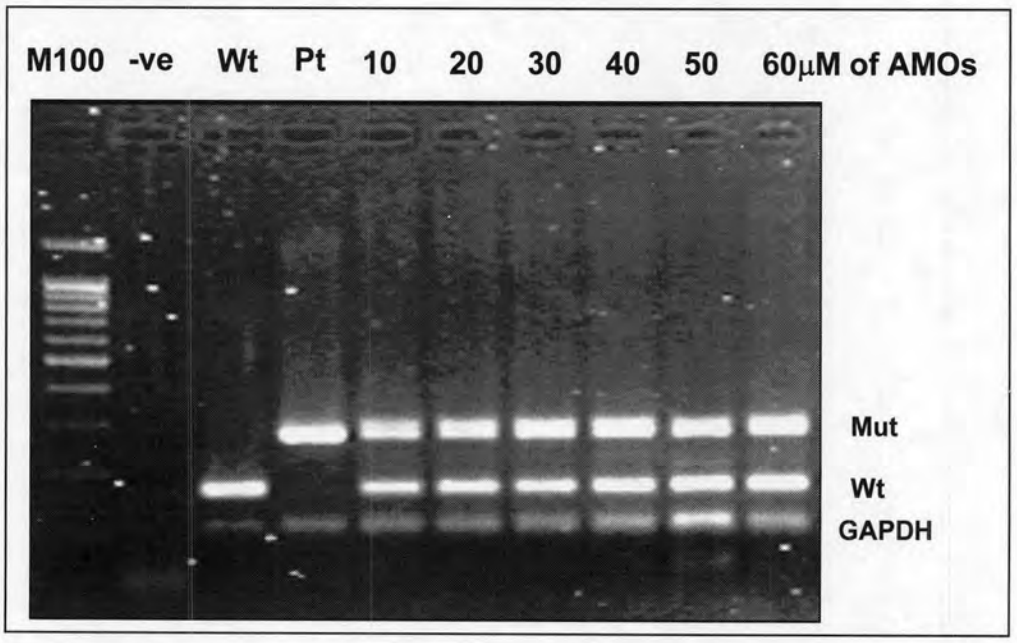

Figure 21: An RT-PCR analysis of the *BTK*-mutated PBMCs treated with various concentrations of target AMOs (10 to 60 μM). -ve = no template control; Wt represents an unaffected control; Pt represents the patient's PBMCs without AMOs treatment

As a result, 10 to 60 μM of AMOs were shown not much different in the levels of correctly spliced *BTK* mRNA. So we treated the *BTK*-mutated PBMCs with lower concentrations of target AMOs (2 and 5 μM) for 24h. The RT-PCR experiments showed dose-dependent correction of splicing (fig.23) Low level of a wide-type product was detected with 2 μM of AMOs but not with 5 μM of AMOs.

Figure 22: An RT-PCR analysis of the *BTK*-mutated PBMCs treated with 2 and 5 µM of target AMOs. -ve = no template control; Wt represents an unaffected control; Pt represents the patient's PBMCs without AMOs treatment

2.4 Duration of an effect of AMOs.

To test the stability of restored, correctly spliced *BTK* mRNA, PBMCs were treated with 10µM of AMOs and were harvested starting at day 1 to day 30. In this experiment, the correction of spliced mRNA was still obtained at day 30 (Fig. 23).

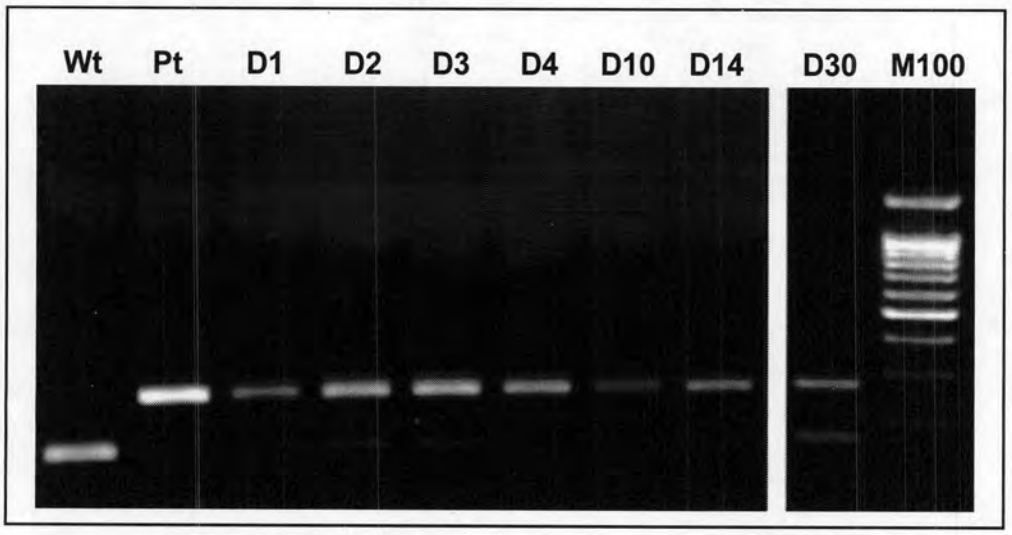

Figure 23: Duration of effect of the target AMOs on aberrant splicing correction, PBMCs derived from the patient were treated with mutation-specific AMOs with a concentration of 10µM and RT-PCR analysis was performed for up to 30 days. Upper band = the mutant PCR product; lower band = the wide-type PCR product

2.5 Specificity of target AMOs

To test the specificity of the target AMOs treatment, the control AMOs, InvertIVS3 were used. Administration with InvertIVS3 control (table 4) did not produce a correct *BTK* mRNA (Fig. 24). The invert AMOs are the 5'→3' invert of the 3' splice site blocker (target AMOs). Administration of the MISIVS3 control could produce a normal *BTK* mRNA.

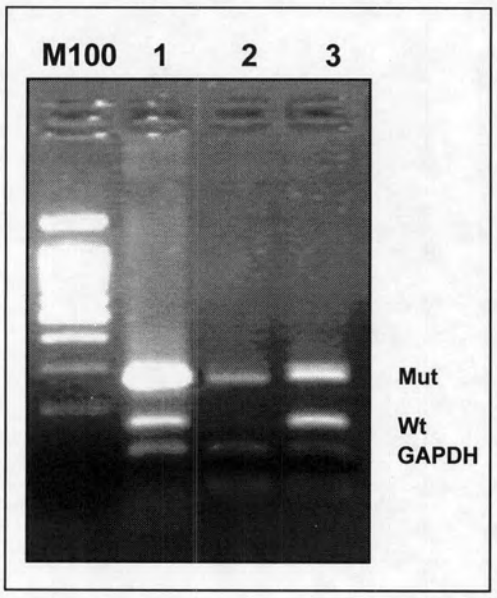

Figure 24: Cells were treated with 10 μM of target AMOs (lane 1) or the control AMOs for 24 h, lane 2 for the InvertIVS3 and lane 3 for the MISIVS3